Desynchronization of pulse-coupled integrate-and-fire neurons

S. Coombes and G. J. Lord
Department of Engineering Mathematics, Bristol University, University Walk, Bristol, BS8 1TR, United Kingdom
(Received 28 October 1996)

Bifurcation analysis of two pulse-coupled integrate-and-fire neurons is used to determine the importance of pulse width, propagation delay, and *shunting* for periodic firing patterns. In contrast to models lacking these simple biological features, stable asynchronous behavior is easily established for reciprocal excitatory coupling between neurons. [S1063-651X(97)50103-6]

PACS number(s): 87.10.+e, 02.30.Ks, 47.20.Ky

The nonlinear dynamics of coupled oscillators consisting of biologically plausible neuron models has recently attracted much interest in neurobiology due to the discovery of synchronized oscillations in the cat visual cortex [1]. Moreover, many biological rhythms, ranging from breathing to walking, are programmed in part by central pattern generating (CPG) networks built from neurons. In many cases, reciprocal synaptic connections between pools of interneurons exist and asynchronous rather than synchronous behavior is the norm [2]. The rhythmic activity of such networks results from an interplay of synaptic interactions and intrinsic membrane properties, belying the need for any persistent external influences. Much of the theoretical work in this area uses the analysis of phase-coupled oscillators developed by Kuramoto [3]. Typically, however, no direct link with electrophysiological data obtained at the cellular level is made. Hence, the role of intrinsic neuromodulation in rhythmic pattern generation cannot be uncovered from such an analysis. Furthermore, neurons (often quiescent in isolation) are modeled as intrinsic oscillators, interacting weakly via their phase differences rather than signaling with action potentials.

Modeling the dynamics of biologically realistic pulse-coupled neurons in which details of individual spikes are included has recently received much attention (see [4] for a review). The integrate-and-fire neuron may be regarded as an abstraction that captures the essentials of a *spiking* neuron [5]. Indeed, it has been shown that a globally pulse-coupled population of such neurons with excitatory synaptic connections always synchronizes with zero phase difference [6–8]. However, in real neurons, spike communication is not instantaneous. The extension of the Mirollo and Strogatz return map formalism [6] has recently been extended to incorporate the effect of small transmission delays [9,10]. Interestingly, for excitatory *spike* coupling, the presence of delays can lead to desychronization. This particular analysis lacks the important notion that the effective input current to a postsynaptic cell has some temporal duration due to the synaptic transmission process. Once again, the inclusion of synaptic currents with realistic rise and fall times can lead to asynchronous behavior in a pair of pulse-coupled integrate-and-fire neurons [11]. Hence, there is growing evidence that the inclusion of more biologically plausible detail into the integrate-and-fire neuron model can have important consequences for modeling neurobiological CPGs.

A further level of well established neurobiological reality that is missing from these integrate-and-fire models is the effect of *shunting* currents. Real neurons possess voltage dependent ionic currents with specific membrane reversal potentials. The incorporation of such currents induces a time dependent cell membrane decay for an integrate-and-fire neuron. In this Rapid Communication we propose to analyze the consequences of such temporal cell membrane properties, in conjunction with realistic postsynaptic currents. Moreover, we incorporate axonal propagation times and extend the work in [9,10] to the case of arbitrary delays. Specifically we show that intrinsic modulation of parameters representing all three of these biological features can lead to stable asynchronous behavior in a pulse-coupled system of two integrate-and-fire neurons with excitatory synapses. To generate oscillations in a system with inhibitory coupling requires an extra physiological factor such as post-inhibitory rebound [12] or the inclusion of an external driving current. A more detailed account of this work, together with a study of electrical synapses and the effects of dendritic structure will be presented elsewhere.

In detail, we consider two identical integrate-and-fire neurons with mutual excitatory coupling. The state variable ϕ_i, $i=1,2$, is used to represent the cell membrane potential at neuron 1 and 2, respectively. Leakage currents drive ϕ_i toward a value that depends upon the synaptic input current and some resting potential (taken as 0). Cell membrane properties determine a time constant τ for each neuron. The neurons are assumed to fire whenever ϕ_i reaches some threshold h, after which ϕ_i is reset to some level $\bar{\phi}$. At this time, the effect of firing is communicated as a spike of electrochemical activity. When this spike arrives at a synapse, neurotransmitter is released and triggers a current in the postsynaptic cell. By denoting the time at which neuron i fires for the nth occasion as T_n^i, the potentials ϕ_i evolve according to the linear ordinary differential equation

$$\frac{d\phi_i}{dt} = -\frac{\phi_i}{\tau} + I_i(t)(s-\phi_i), \quad t \in (T_n^i, T_{n+1}^i) \tag{1}$$

with the strongly nonlinear reset conditions

$$\lim_{\epsilon \to 0_+} \phi_i(T_k^i - \epsilon) = h, \quad \lim_{\epsilon \to 0_+} \phi_i(T_k^i + \epsilon) = \bar{\phi}. \tag{2}$$

Here, $I_i(t)(s-\phi_i)$ represents the *shunting* synaptic input current from neuron j to neuron i. The membrane reversal potential, s, is positive for an excitatory synapse and nega-

tive for an inhibitory one. The extension of (1) to larger populations than two is easily achieved, but at the expense of analytical tractability. However, large coupled populations of the type (1) simplify considerably when τ is much larger than the mean interspike interval and *shunting* terms are dropped. In this case a Lyapunov function exists and a discussion of the rate of approach to periodic solutions is possible [13]. Furthermore, an analysis of the effect of delays is also possible under these assumptions [14].

We restrict attention to the case in which the coupled system (1) fires with a period Δ and relative phase θ and choose the times at which neuron 1 and 2 last fired as 0 and $-\theta\Delta$, respectively. For example, we may now write the input to neuron 2 as a sum of delayed pulse functions

$$I_2(t)=\sum_{n\to-\infty}^{0} H(t-n\Delta-t_d) \tag{3}$$

with t_d representing some axonal propagation delay time. Choosing a biologically plausible pulse shape such as the α function [15], $H(t)=g\alpha^2 te^{-\alpha t}$, the infinite sum in (3) reduces to a convergent geometric progression such that $I_2(t)=I(t)$ with $t\in[t_d,t_d+\Delta)$ and $I(t)$ periodic in Δ such that

$$I(t)=\frac{g\alpha^2 e^{-\alpha(t-t_d)}}{(1-e^{-\alpha\Delta})}\left\{(t-t_d)+\frac{\Delta e^{-\alpha\Delta}}{(1-e^{-\alpha\Delta})}\right\}. \tag{4}$$

In a similar fashion one may establish that $I_1(t)=I(t+\theta\Delta)$. The evolution of the membrane potentials in a periodic firing pattern, $\phi_i(t+n\Delta)=\phi_i(t)$, $n\in\mathbb{Z}$, now takes the form

$$\frac{d\phi_i}{dt}=A_i(t)\phi_i+F_i(t),\quad t\in(0,\Delta) \tag{5}$$

with

$$A_i(t)=-\frac{1}{\tau}-I(t+\eta_i\theta\Delta),\quad F_i(t)=sI(t+\eta_i\theta\Delta) \tag{6}$$

and $\eta_1=+1$ and $\eta_2=-1$. The quantities $A_i(t)$ may be regarded as time dependent cell membrane decay functions. For a single neuron receiving constant high rates of spike stimulation, the effective cell membrane decay rate is increased so that the steady state value of cell membrane potential is lower than would occur in the absence of shunting. Hence, in this context shunts can act to limit the firing rate of a neuron.

The formal solution of (5) is

$$\phi_i(t)=\int_0^t G_i(t,t')F_i(t')dt', \tag{7}$$

$$G_i(t,t')=\exp\int_{t'}^{t}A_i(t'')dt'',\quad t\in(0,\Delta) \tag{8}$$

(with $\overline{\phi}=0$ for simplicity). The self-consistent solution of the equations for the somatic potentials given by (7) and (8) determines both the phase and period for the steady state periodic behavior. Two obvious phase solutions are $\theta=0$ (or equivalently $\theta=1$) and $\theta=1/2$. Moreover, if θ is a solution, then $(1-\theta)$ is also a solution.

A simple condition on the phase and period is formed from the expression

$$\mathcal{G}(\theta,\Delta)=\phi_1(\Delta)-\phi_2(\Delta)=0 \tag{9}$$

and hence $\phi_2(\Delta)=h-\mathcal{G}(\theta,\Delta)$. To determine the stability of a given solution suppose that θ is slightly larger than a stable equilibrium value. Then neuron 2 should fire later to restore the correct value of θ. This requires that $\phi_2(\Delta)$ be smaller than h, or equivalently, that $\mathcal{G}(\theta,\Delta)$ should be an increasing function of θ near the equilibrium value. Otherwise a reset will occur, causing a dramatic change in the network dynamics. Hence, the condition for stability of a solution is defined by

$$\frac{\partial\mathcal{G}(\theta,\Delta)}{\partial\theta}>0. \tag{10}$$

Bifurcation diagrams are produced using AUTO94 [16], a numerical continuation code for differential and algebraic equations. The code implements Keller's pseudo-arclength continuation and in particular for algebraic systems such as considered here:

$$\phi_i(\Delta)-h=0,\quad i=1,2 \tag{11}$$

detects simple bifurcations and performs branch switching. Note that due to the solution structure of the ϕ_i, each of the equations in (11) is in fact an integral equation. The use of numerical quadrature allows the reduction of the two integral equations to two nonlinear algebraic ones. For the purposes of this Rapid Communication a standard composite Simpson's rule was chosen for evaluation of all integrals. All

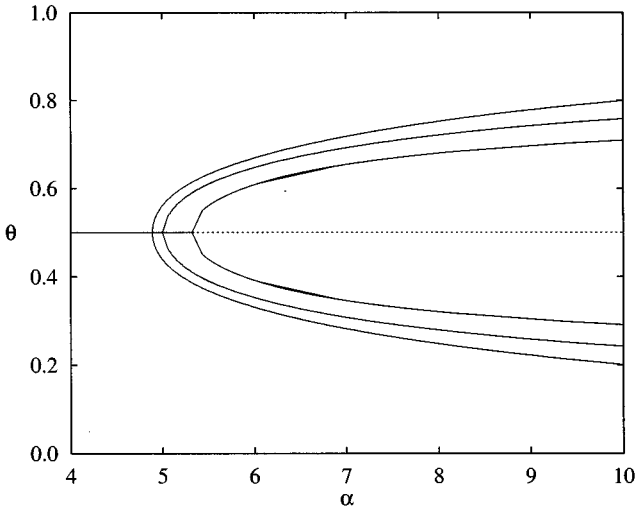

FIG. 1. Bifurcation diagram of θ vs α with $s=1$. The three branches above and below the antisynchronous state ($\theta=1/2$) correspond to three differing values of the time delay t_d. The branch bifurcating from $\theta=1/2$ at the lowest value of α corresponds to the case with no delay, $t_d=0$. Successive bifurcations for progressively larger α correspond to the case with delays, $t_d=0.0025$ and $t_d=0.1$, respectively. Solid (dashed) lines represent stable (unstable) solutions.

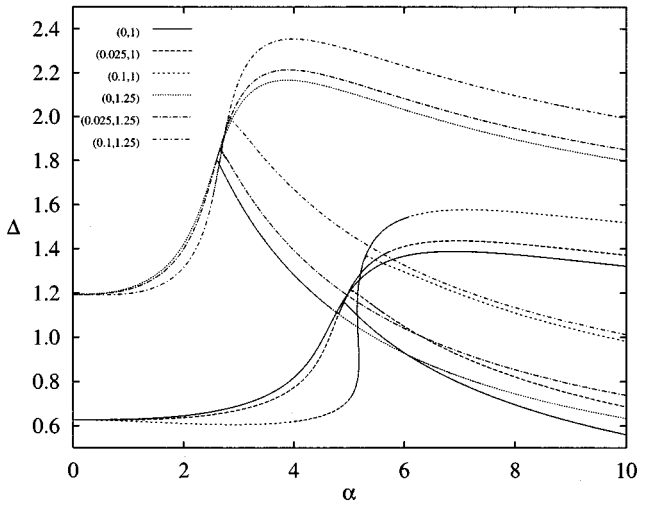

FIG. 2. Bifurcation diagram of Δ vs α. Line key defined with (t_d, s). The upper set of curves correspond to a system with stronger shunting current than the lower set. Each set is plotted with three varying delays defined in the key. Beyond the bifurcation point (for each (t_d, s), α increasing) a new asynchronous solution (with a lower value of Δ) appears, born from the antisynchronous solution shown.

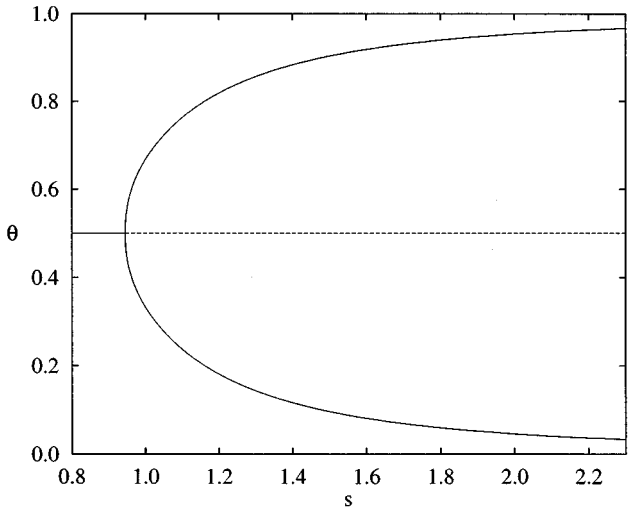

FIG. 3. Bifurcation diagram of θ vs s for $t_d=0$ and $\alpha=6$. Solid (dashed) lines represent stable (unstable) solutions.

computations were performed with $g=0.4$, $h=0.25$ and a time scale was chosen such that $\tau=1$.

For small values of the synaptic rate constant α there are two possible states showing either complete *synchrony*, $\theta=0,1$, or *antisynchrony*, $\theta=1/2$ (see Fig. 1). Only the antisynchronous state is stable. With increasing α, corresponding to progressively faster synapses, there is a pitchfork bifurcation at a critical value of $\alpha=\alpha^c$ and two additional equilibria are born. The antisynchronous solution loses stability and continues as an unstable branch. The two new states are stable and have intermediate phases, i.e., are neither synchronous nor antisynchronous and will be termed asynchronous. Also shown in this figure are phase solutions in the presence of small delays ($t_d \leqslant 0.1$). Once again there is a pitchfork bifurcation from a stable antisynchronous solution leading to the creation of two new stable states for some critical α. Note, however, that in comparison to the solutions with zero delay, *desynchronization* occurs. With increasing t_d, α_c occurs at progressively larger values and for $\alpha > \alpha_c$ solution branches move closer to the antisynchronous solution. In Fig. 2 we explicitly follow the antisynchronous solution and plot the period of oscillation, Δ, for both this solution and the asynchronous one that is born from it at α_c. The lower set of curves in Fig. 2 corresponds to a system with weaker shunting currents than those plotted above. This confirms the idea that shunts can act to limit the firing frequency of the two neuron system. Furthermore, delays lead to a decrease in the period Δ for $\alpha < \alpha_c$ and an increase in the period of all solutions with $\alpha > \alpha_c$, for a fixed value of s.

There is also a pitchfork bifurcation in the phase θ as a function of the shunt parameter s. For s less than some critical value s_c the system fails to oscillate since the threshold condition can never be reached in this parameter regime. With $s > s_c$ three solutions exist, and for larger values of s two new stable solutions are created. For small delays ($t_d < 0.075$) the bifurcation point and branches shown in Fig. 3 do not vary significantly. Larger delays, however, lead to a more complex bifurcation picture which will be presented in further work. Interestingly, for a large range of s and α, the presence of delays leads to the existence of multiple stable solutions with the same phase but differing period. Note that multistable dynamical systems have important applications as pattern recognition and memory storage devices.

In the limit $\alpha \to \infty$ a α function approximates the δ pulse shape considered in the seminal work of Mirollo and Strogatz [6]. In the absence of shunting currents and time delays, the only stable periodic solution is the synchronous one as expected. Importantly, however, we have shown, with realistic forms of postsynaptic current, that the introduction of shunts and the presence of even arbitrarily small delays leads to the creation of a stable asynchronous solution. With the inclusion of an external input, $I_0 > h/\tau$, an integrate-and-fire neuron intrinsically oscillates and rhythmic behavior is possible in a purely inhibitory network. In this case bifurcation diagrams are qualitatively the same as those presented here, but with a reversal of stability for all solution branches.

[1] W. Singer, in *The Handbook of Brain Theory and Neural Networks*, edited by M. A. Arbib (MIT Press, Cambridge, 1995), pp. 960–963.

[2] R. L. Calabrese, in *The Handbook of Brain Theory and Neural Networks*, edited by M. A. Arbib (MIT Press, Cambridge, 1995), pp. 444–447.

[3] Y. Kuramoto, *Chemical Oscillations, Waves and Turbulence* (Springer-Verlag, New York, 1984).

[4] W. Gerstner, Phys. Rev. E **51**, 738 (1995).
[5] L. F. Abbott and T. B. Kepler, in *Statistical Mechanics of Neural Networks*, edited by L. Garrido (Springer-Verlag, Berlin, 1990).
[6] R. E. Mirollo and S. H. Strogatz, SIAM (Soc. Ind. Appl. Math.) J. Appl. Math. **50**, 1645 (1990).
[7] Y. Kuramoto, Physica D **50**, 15 (1991).
[8] S. Bottani, Phys. Rev. Lett. **74**, 4189 (1995).
[9] U. Ernst, K. Pawelzik, and T. Geisel, Phys. Rev. Lett. **74**, 1570 (1995).
[10] R. Mather and J. Mattfeldt, SIAM (Soc. Ind. Appl. Math.) J. Appl. Math. **56**, 1094 (1996).
[11] C. V. Vreeswijk and L. F. Abbott, J. Comput. Neurosci. **1**, 313 (1994).
[12] S. Coombes and S. H. Doole, Phys. Rev. E **54**, 4054 (1996).
[13] A. V. M. Herz (unpublished).
[14] W. Gerstner, Phys. Rev. Lett. **76**, 1755 (1996).
[15] J. J. B. Jack, D. Noble, and R. W. Tsien, *Electric Current Flow in Excitable Cells* (Oxford Science Publications, Oxford, 1975).
[16] E. Doedel, H. B. Keller, and J. P. Kernevez, Int. J. Bifurcation Chaos **1**, 493 (1991).